RSC Advances

PAPER

View Article Online
View Journal | View Issue

Cite this: *RSC Adv.*, 2023, **13**, 22875

Biodegradable Gg-*cl*-poly(NIPAm-*co*-AA)/-*o*-MWCNT based hydrogel for combined drug delivery system of metformin and sodium diclofenac: *in vitro* studies

Pragnesh N. Dave, *[a] Pradip M. Macwan[b] and Bhagvan Kamaliya[a]

In the present study Gg-*cl*-poly(NIPA-*co*-AA) and Gg-*cl*-poly(NIPA-*co*-AA)/-*o*-MWCNT hydrogels were synthesized using free radical polymerization. We looked into whether combining metformin with diclofenac, a nonsteroidal anti-inflammatory drug (NSAID), would be effective in examining complex formation and analysing the types and intensities of complexes that could result from metformin–diclofenac interactions. The interaction of metformin and diclofenac was studied *in vitro* at various pH levels and body temperatures. The structure and morphology of the produced hydrogel were characterised using FTIR spectra, SEM analysis, and drug loading tests. As a model drug, the hydrogel was loaded with metformin hydrochloride and sodium diclofenac (DS), and the medicines were released pH-dependently. To explore the drug release kinetics and mechanism, the zero order and first order kinetic models, the Korsemeyar–Peppas model, the Higuchi model, and the Hixson-Crowell model have all been employed. Drug release studies revealed notable characteristics in connection to physiologically predicted pH values, with a high release rate at pH = 9.2. At pH = 9.2, however, both metformin and sodium diclofenac exhibited a Fickian mechanism. Combination treatment may reduce the effective dose of a single drug and hinder metabolic rescue mechanisms. More study is needed to detect any negative effects on individuals.

Received 14th July 2023
Accepted 24th July 2023

DOI: 10.1039/d3ra04728h

rsc.li/rsc-advances

1. Introduction

Hydrogels are copolymeric networks that can expand and retain water inside their polymeric network while not dissolving in water.[1] Graft copolymers provide advantages over natural polymers, particularly stimuli-responsive polymers, such as greater acid base and heat resistance and decreased crystallinity. Graft copolymers are made by first generating free radicals on the biopolymer backbone and then allowing these radicals to act as macroinitiators.[2] Hydrogels have a longer and more persistent effect than traditional drug delivery techniques. They are biocompatible and biodegradable, and they administer drugs to particular locations. As a result of the reduced frequency of dose and adverse effects, patient compliance improves.

Natural polymers have been widely used as drug entrapment and delivery vehicles.[3,4] Natural polymers outperform synthetic polymers in terms of biocompatibility, biodegradability, and ease of access.[3,5] Additionally, the presence of reactive groups on native natural polymers allows for interaction with other functional groups.[6] This modification bestows amazing functionalities on the newly acquired polymer and/or affects its physical and chemical characteristics.[7,8] Graft copolymerization methods have attracted a lot of interest for their ability to modify natural polymers.[9–11] This approach allows for the grafting of one or more homopolymer blocks with a variety of functional groups onto the main chain's backbone, modifying the physical and chemical characteristics of the original grafted polymer.[10] Graft polymerization may be accomplished in three ways: grafting to, grafting from, and grafting through. The "grafting to" method involves the coupling of a pre-formed polymer to a surface by using the functional groups of both the surface and the pre-formed polymer.[6]

The principle behind the drugs delivery technology is based on the premise that every pharmaceutical dosage form should be designed to deliver therapeutic amounts of drugs to the site of action and maintain them during therapy.[12] Because of their efficacy as anti-inflammatory, anti-thrombotic, anti-pyretic, and analgesic agents, nonsteroidal anti-inflammatory medicines (NSAIDs) are among the most regularly prescribed pharmaceuticals in the world. Numerous adverse drug responses, case-control, and post-marketing monitoring studies, however, have demonstrated that NSAIDs are linked with a wide range of side effects, the most common of which are gastrointestinal (GI) problems.

[a]*Department of Chemistry, Sardar Patel University, Vallabh Vidyangar, Gujarat 388 120, India. E-mail: pragnesh7@yahoo.com*

[b]*B. N. Patel Institute of Paramedical & Science (Science Division), Sardar Patel Education Trust, Bhalej Road, Anand 388001, Gujarat, India*

Diclofenac is a well-tolerated nonsteroidal anti-inflammatory drug (NSAID) that is commonly used in the long-term treatment of degenerative disorders such as rheumatoid arthritis and osteoarthritis.[13] The drug also has analgesic and antipyretic properties. However, due of its short biological half-life (1–2 h), it must be administered often to maintain therapeutic efficacy. The use of drug-delivery devices is one possible approach to discovering a successful therapy employing sodium diclofenac. More precisely, drug delivery is a new research path in precision medicine that aims to improve the therapeutic benefits of drugs in people or animals.[14] Metformin hydrochloride ($C_4H_{12}ClN_5$), also known as 1,1-dimethylbuguanide hydrochloride, is a small and very hydrophilic molecule that is commonly employed in the treatment of type 2 diabetes. This drug is usually given to people whose glucose levels cannot be managed *via* diet and exercise.[15] It has three basic functions: reducing sugar absorption in the small intestine, stopping the liver from excreting more glucose into the blood, and eventually supporting the body in using natural insulin properly. As a result, it reduces endogenous glucose synthesis while causing no obvious hypoglycemia. However, because it is hydrophilic, it is only partly and slowly absorbed by the gastrointestinal system, resulting in a relatively poor bioavailability (50–60%). Furthermore, because metformin HCl has a very short half-life (2–4 h), frequent medication administration is required for successful management.[6]

Because both stimuli are created in the mammal's body, temperature and/or pH sensitive gels are the most studied for drug delivery applications.[16–18] *N*-isopropylacrylamide (NIPAm) is the most studied thermos-responsive gel polymer. Poly(*N*-isopropylacrylamide) [poly(NIPAm)] hydrogels have an enlarged network structure below 32 °C, the lower critical swelling temperature (LCST),[19] whereas these networks collapse above this temperature. Cross-linked and poly(acrylic acid) [poly(AAc)] hydrogels, on the other hand, are the most pH sensitive materials studied because they can exhibit much more expanded networks at pH values above the pK_a of acrylic acid (pK_a = 4.35) and the changes in network expansion are in the range close to the body's pH. Because of established features such as excellent mucoadhesion, ionic drug load possibility, high swelling, and biocompatibility, certain materials based only on acrylic acid (as carbopol derivatives) are frequently employed to construct pharmaceutical drug delivery formulations. However, the use of this monomer in combination with NIPAm can provide polymer-drug based formulations with additional benefits such as (a) slower rate of drug release at body temperatures compared to polymers completely based on AAc due to their partially collapsed state at body temperature and (b) improvement of mechanical properties of the formulations due to major polymer–polymer interactions.[20]

To address these issues, an effort was made to develop hydrogel composites based on gum ghatti with an interpenetrating network using free radical copolymerization and a cross linker-initiator system consisting of *N*,*N*′-methylene-bisacrylamide (MBA) and ammonium peroxydisulfate (APS), *N*-isopropylacrylamide, and tetramethylethylenediamine (TEMED) as an initiator. The current study's major purpose was to investigate complex formation and analyse the types and severity of complexes that might occur from metformin and diclofenac interactions.

2. Materials and methods

2.1. Materials

Gum ghatti (Gg), acrylic acid (AA), ammonium persulfate (APS), tetramethyl ethylenediamine (TEMED) and *N*,*N*′-methylenebisacrylamide (MBA) were purchased from Lobachemie (Mumbai, India). *N*-isopropylacrylamide (NIPAm) was purchased from TCI. -*o*-MWCNT was directly used as per our previous work.[21] Metformin hydrochloride (CAS number: 1115-70-4) was purchased from Himedia and Sodium diclofenac (SD) (CAS number: 15307-79-6) was purchased from Sigma Aldrich. The structure of the model drugs are given below as Fig. 1. All reagents used were of analytical grade. For all the experiments, deionized (DI) water was used.

2.2. Synthesis of gum ghatti-*cl*-poly(*N*-isopropylacrylamide-*co*-acrylic acid)/-*o*-MWCNT

Gg-*cl*-poly(NIPA-*co*-AA)/-*o*-MWCNT hydrogels were synthesized by adding 0.5 g Gg to 10 ml of distilled water in a 100 ml beaker and kept in rest for 24 h for better dissolution of the biopolymer in water. The composition was sonicated for 40 minutes and after that -*o*-MWCNT (0–50 mg) solution was added to biopolymer. To the beaker 0.2 gm of NIPAm was added and the

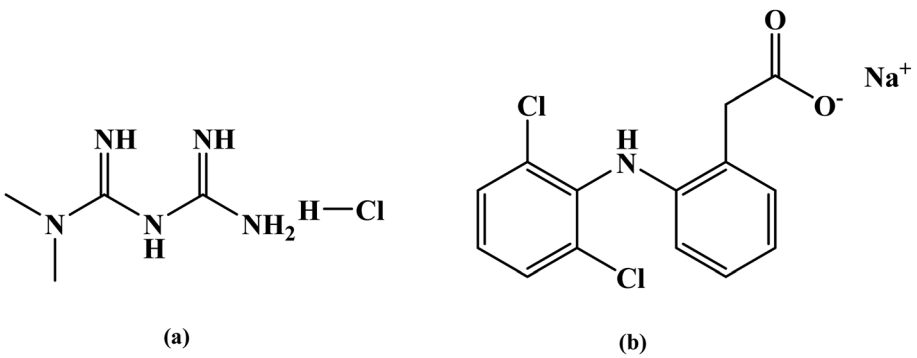

Fig. 1 Chemical structures of (a) metformin hydrochloride and (b) sodium diclofenac drug.

Table 1 Experimental conditions to yield hydrogels

S. no.	Gum ghatti (g)	NIPAm (g)	AA (ml)	APS (g)	MBA (g)	TEMED (ml)	-*o*-MWCNT (mg)	H_2O (ml)
GNACNT-0	0.5	0.2	1	0.05	0.05	0.05	0.0	10
GNACNT-1	0.5	0.2	1	0.05	0.05	0.05	10	10
GNACNT-2	0.5	0.2	1	0.05	0.05	0.05	20	10
GNACNT-3	0.5	0.2	1	0.05	0.05	0.05	30	10
GNACNT-4	0.5	0.2	1	0.05	0.05	0.05	40	10
GNACNT-5	0.5	0.2	1	0.05	0.05	0.05	50	10

required amounts of APS, TEMED and MBA was added as shown in the Table 1. In the final phase, 1 ml of AA was added with constant stirring. The beaker was left undisturbed at 50 °C for 3 h. After 3 h, the beaker was allowed to cool at room temperature. The formed homo-polymer was extracted using repeated acetone extractions. The hydrogel was allowed to dry gradually at 50 °C for 48 h and grounded into powder with a mortar and pestle.

2.3. Characterization of gum ghatti grafted hydrogel

2.3.1. Fourier transform infrared spectroscopy (FTIR). Fourier transform infrared (FT-IR) spectra of materials were recorded on PerkinElmer instrument using KBr plate method in the range of 400–4000 cm^{-1}.

2.3.2. Surface morphological study (SEM). The morphology of particles was studied utilising SEM studies, which make use of a scanning electron microscope. In this method, a sample is scanned using a high-intensity electron beam. A Field Emission Gun Nano Nova Scanning Electron Microscope (FEG-SEM) 450 with EDAX was used to analyse hydrogels. For sample analysis, magnification levels ranged from ×25 to ×10 000.

2.4. Drug loading study

2.4.1. Loading of metformin and sodium diclofenac onto the hydrogel. The model drugs sodium diclofenac and water-soluble metformin were introduced into hydrogel using a swelling-diffusion method.[22] A 100 ml solution of metformin (1.0 mg ml^{-1}) and sodium diclofenac (1.0 mg ml^{-1}) was transferred to the dried hydrogels (1.0 g), and they were then incubated at 37 °C for 24 hours. After being taken out of the solutions, the combined hydrogels were washed with deionized water and dried in an oven at 50 °C to a constant weight. Using a UV-visible spectrophotometer, the quantities of metformin and sodium diclofenac were determined (Shimadzu-1800). The drug entrapment efficiency (EE) of the hydrogel was determined using the eqn (1) shown below.[23]

$$\mathrm{DL}\ (\%) = \left(\frac{W_{\mathrm{D}}}{W_0}\right) \times 100 \quad (1)$$

where W_{D} is the total amount of drug in solution after loading and W_0 is the total amount of drug in solution before loading.

2.4.2. *In vitro* drug release study. The release behaviour of model drugs from the drug loaded hydrogel (powder type) were investigated in distilled water, at pH 1.2 buffer (simulated stomach fluid), pH 7.4 buffer (simulated intestinal fluid), and pH 9.2 (borate). The calibration curves for the drugs were generated in distilled water, pH 1.2 buffer, pH 7.4 buffer, and pH 9.2 buffer solutions at 232 nm for metformin and 276 nm for sodium diclofenac using a UV-visible spectrophotometer (Shimadzu-1800). The drug-loaded hydrogels were immersed in 100 ml of PBS buffer (pH = 7.4), HCl (pH = 1.2), and borax (pH = 9.2) solutions for the release studies. The experiments were carried out in an incubator at 100 rpm at a working temperature of 37 °C. At predetermined time intervals, a small volume of the release medium (5.0 ml) was taken to determine the drug concentration using a UV-visible spectrophotometer, and an identical volume of new medium was added.

2.4.3. Mechanism of drug release. The release data was fitted in the well-known Korsmeyer–Peppas equation shown below to define the drug release process[24,25]

$$\frac{M_t}{M_\infty} = kt^n \quad (2)$$

where 'k' is a release rate constant characteristic of the structure and geometry of the drug delivery device, 'n' is the diffusion exponent characteristic of the release mechanism, and M_t/M_∞ is the proportion of the drug released at time 't'.[26–28] The values of 'n' and 'k' are obtained from the slope and intercept of the log M_t/M_∞ plot and the log t plot, respectively. Dependent on the comparative rates of water diffusion into the polymer matrix and rate of polymer chain relaxation, there are three different ways that drugs can be released from drug-loaded polymers. For the sample, $n = 0.89$ relates to case II diffusion (the release mechanism is relaxation controlled), $n = 0.45$ relates to Fickian diffusion (the release mechanism is diffusion controlled), and n between 0.45–0.89 relates to non-Fickian diffusion (a mixture of Fickian diffusion and polymer chain relaxation).[29]

2.4.4. Kinetics of drug release. The best fit of the curves to several kinetic models, including the zero order model (eqn (3)), the first order model (eqn (4)), the Higuchi model (eqn (5)), the Korsmeyer–Peppas model (eqn (6)) and the Hixson-Crowell model (eqn (7)) was used to determine the kinetics of drug release from the hydrogel.[30]

$$\frac{M_t}{M_\infty} = k_0 t \quad (3)$$

$$\log\left(\frac{M_t}{M_\infty}\right) = k_1 t \quad (4)$$

$$\left(\frac{M_t}{M_\infty}\right) = k_2 t^{\frac{1}{2}} \quad (5)$$

$$\left(\frac{M_t}{M_\infty}\right) = k_3 t^n \quad (6)$$

$$\sqrt[3]{M_0} - \sqrt[3]{M_t} = k_4 t \quad (7)$$

In the above stated models M_t/M_∞ is the cumulative fraction of drug release, 't' is the release time, 'n' is the release exponent, M_0 is the amount of drug loaded in hydrogel, M_t is amount of drug release at time 't' and k_0, k_1, k_2, k_3 and k_4 are the release rate constants.[31]

3. Results and discussion

3.1. Fourier transform infrared spectroscopy (FTIR spectroscopy)

Fig. 2 displays the FTIR spectra for gum ghatti-*cl*-poly(*N*-isopropylacrylamide-*co*-acrylic acid)/-*o*-MWCNT hydrogel. Gum ghatti showed a wide absorption band at 3419.61 cm^{-1} because of the presence of –OH in galactopyranose and glucopyranose rings, a peak at 2925.26 cm^{-1} arises because of the C–H stretching mode of the $-CH_2$ group, and peak at 1628.66 cm^{-1} is because of the C=O stretching vibrations. It was determined that the pyranose rings of polysaccharides C–O and C–C stretching vibrations were responsible for the absorption peaks between 1033.08 cm^{-1} and 1421.97 cm^{-1}. The peaks at 1311.47 cm^{-1} and 1234.70 cm^{-1} were caused by stretching vibrations of the C–O–C.[32] The bands due to the C=O stretch are very prominently seen in the range 1710.48 cm^{-1} for the carboxylated MWCNT, which can be assigned to the acid carbonyl-stretching mode.[33] Apart from this, other bands seen in this *o*-MWCNT are a small one at 2824.03 cm^{-1} and another at 3331.87 cm^{-1}, that are characteristic of C–H and O–H, stretches respectively.[34] The bands at 1287.84 cm^{-1} and 1404.26 cm^{-1} are representative of C=C.[35] It can also be observed that, the intensity of this O–H peak is relatively lower and shows that a lesser amount of amorphous carbon formed during growth.[33] It is well known than an acid treatment with HNO_3 allowed the introduction of carboxyl groups onto the surfaces of the MWCNTs.

The O–H stretching from the carboxylic group is responsible for the noticeable peak at 3444.07 cm^{-1}. The peak at 3004.55 cm^{-1} is caused by N–H bending vibration from the NIPAm-$CONH_2$ group. Furthermore, the distinctive peak at 1673.37 cm^{-1} is due to C=O stretching of the carboxylic acid group of PAA, and the peak at 1580.57 cm^{-1} is due to NIPAm C=O stretching. The aromatic C=C stretching vibration causes the peak at 1432.94 cm^{-1}, whereas the C–N stretching vibration causes the peak at 1208.55 cm^{-1}. Chen *et al.*[36] labelled the stretching vibration of $-CH_2$ and –CH in the range of 2973–2975 cm^{-1}, but no peak in this region was found for Gg-*cl*-poly(NIPAm-*co*-AA), but two peaks emerged at 2706 and a small peak at 2848.49 cm^{-1} that could be designated to stretching vibration of $-CH_2$ and –CH respectively present in the Gg-*cl*-poly(NIPAm-*co*-AA). The results show that a gum ghatti-*cl*-poly(NIPAm-*co*-AA) hydrogel was formed. A pure sodium diclofenac drug molecule also exhibits a doublet of amine groups. Similar to the band at 1579.73 cm^{-1} ascribed to the carbonyl group, this wide band may be the result of the interaction of the –NH group with the –OH group.[37,38] The bands at 1579.73, 1497.90, 1263.38, 1048.27 and 663.59 cm^{-1} corresponding to the C=C group of aromatic ring, C–N stretching and C–Cl group.[39] All of the bands found in the drug molecule as well as the newly formed functional groups C–O–C and hydrogen connected –NH may be seen in the FTIR spectra of a drug-loaded hydrogel.[40]

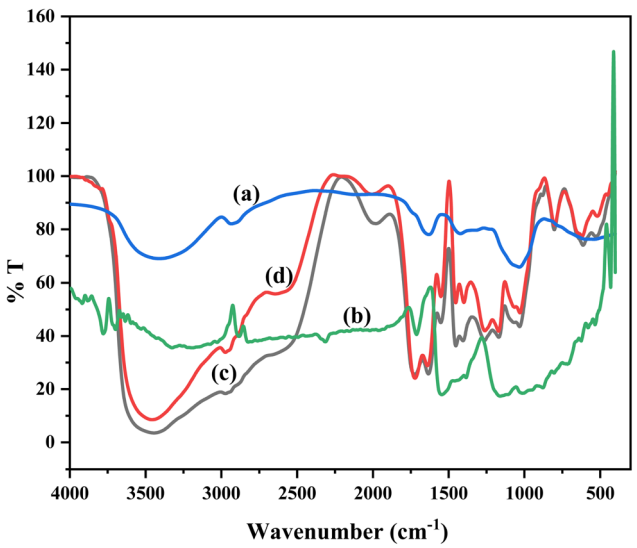

Fig. 2 FT-IR spectra for (a) pure gum ghatti (Gg), (b) pure -*o*-MWCNT, (c) GNACNT-0 hydrogel, (d) GNACNT-3 drug loaded hydrogel.

3.2. Scanning electron microscopy (SEM)

Fig. 3a demonstrates the SEM examination of pure gum ghatti (Fig. 3a). SEM of the pure gum ghatti indicated the presence of polyhedral flakes with a rough surface morphology. Fig. 3 displays SEM images of hydrogels made from gum ghatti-*cl*-poly(NIPA-*co*-AA), -*o*-MWCNT, and gum ghatti-*cl*-poly(NIPA-*co*-AA)/-*o*-MWCNT. Due to abrasion and disassembly, the -*o*-MWCNT has a multi-layered, disordered structure and the surface of the oxidized MWCNTs looks rough because of the defected regions created by oxidation, as shown in Fig. 3b. The surface morphology of the hydrogel without -*o*-MWCNT seems rough, but it gets smooth with -*o*-MWCNT. The -*o*-MWCNT particles may operate as a nucleating centre over which the polymer develops at a constant rate. The agglomerated structures were formed because of the addition of -*o*-MWCNT. The surface of the oxidized MWCNTs looks rough because of the defected regions created by oxidation (Fig. 3b). In comparison to the neat gum ghatti (Fig. 3b), surface morphology of both the hydrogel and its nanocomposite exhibits almost peeled smooth combined with rough irregular surface morphology shown in (Fig. 3b). Impregnation of -*o*-MWCNTs within the from gum ghatti-*cl*-poly(NIPA-*co*-AA) hydrogel polymer matrix leads to the appearance of the white layer on the peeled smooth (Fig. 3c). While, it can be clear from SEM images that the -*o*-MWCNT

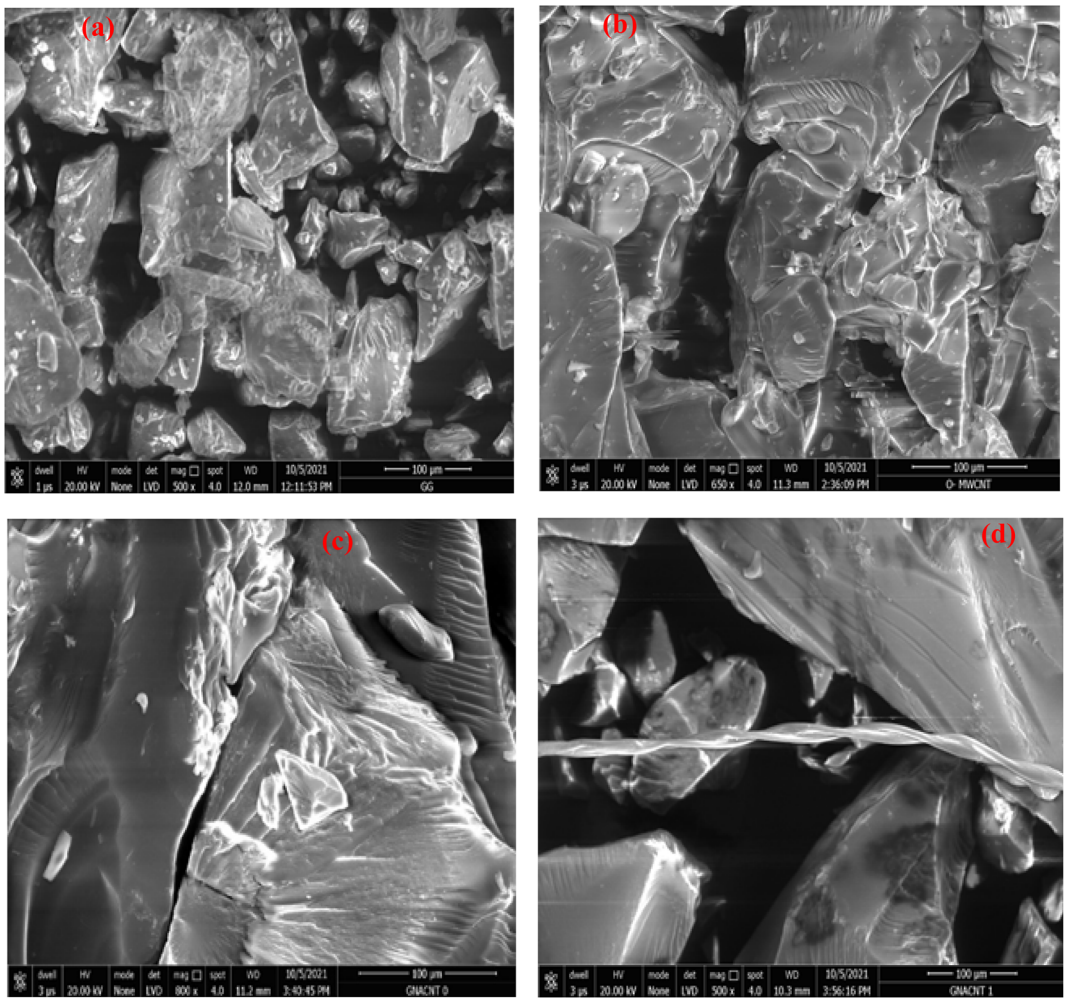

Fig. 3 SEM images for (a) pure gum ghatti, (b) -*o*-MWCNT and (c) GNACNT-0 hydrogel and (d) GNACNT-1 hydrogel.

loaded hydrogel (Fig. 3d), morphology is entirely different from unloaded hydrogel (Fig. 3c) and show packing of -*o*-MWCNT on to hydrogel surface. Similar observation can also be observed between -*o*-MWCNT loaded hydrogel nanocomposite and unloaded hydrogel nanocomposite (Fig. 3d). This suggested that -*o*-MWCNT was responsible for causing the scattered phase to agglomerate.

3.3. Drug loading efficiency

The model drug of metformin and sodium diclofenac loaded onto hydrogel (GNACNT-0, GNACNT-1 and GNAGO-3) is depicted in Table 2 below.

Table 2 Percentage drug loading of GNACNT-0, GNACNT-1 and GNAGO-3 hydrogels at fixed temperature and fixed pH values

Sample code	Temp. (°C)	pH	Metformin drug loaded (%)	Sodium diclofenac drug loaded (%)
GNACNT-0	30	6.8	98.28	99.40
GNACNT-1	30	6.8	98.22	99.42
GNACNT-3	30	6.8	98.33	99.30

From the above table (Table 2) it can be seen that the drug loading efficiency of the synthesized GNACNT-0, GNACNT-1 and GNACNT-3 hydrogel is 98.28%, 98.22% and 98.33% for metformin while for sodium diclofenac drug for the same hydrogel is 99.40%, 99.42% and 99.30% at 30 °C temperature and pH of 6.8.

Hydrophilic chains were found in the synthesized GNACNT hydrogels. These chains help in the easy sliding of the drug molecules in the synthesised GNACNT matrix, resulting in easy drug loading into the matrix. These groups are also helpful in the simple dissolution and diffusion of the drug through the matrix. Because the synthesised GNACNT hydrogel swelled continuously as a function of time, it has been found to be an appropriate approach for controlled drug release. As releasing medium, pH solutions of 1.2, 7.4, and 9.2 were utilised. The drug release behaviour was investigated at various pH levels.

3.4. *In vitro* drug release study

3.4.1. Effect of pH on metformin HCl and sodium diclofenac drug release. The release profile of metformin and sodium diclofenac model drugs was investigated using

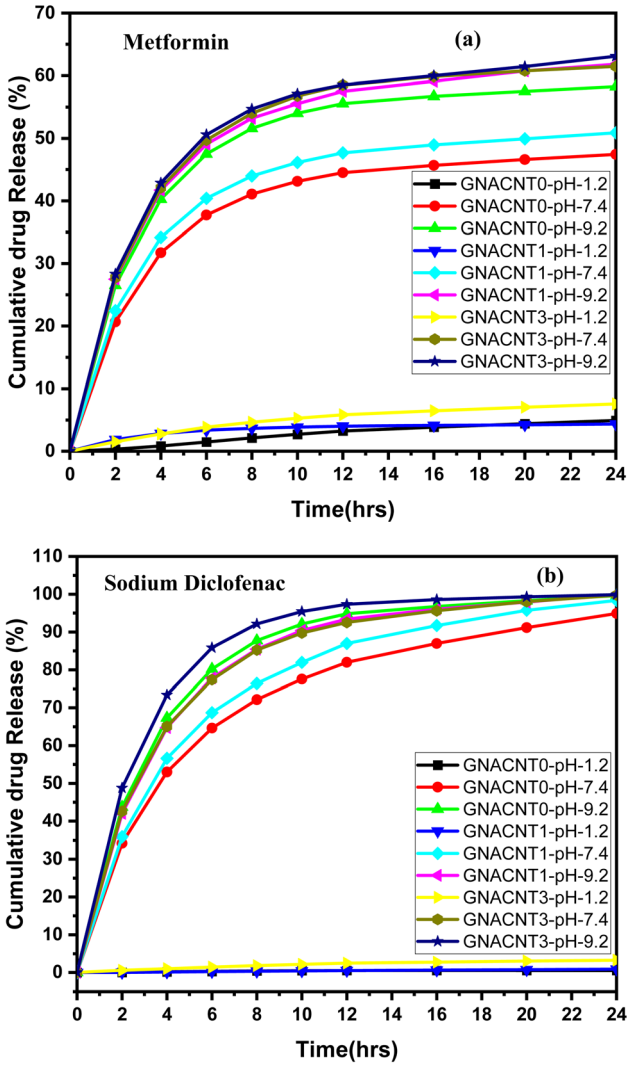

Fig. 4 Cumulative drug release *versus* time plot for (a) metformin HCl and (b) sodium diclofenac drug loaded GNACNT-0, GNACNT-1 and GNACNT-3 hydrogels at pH = 1.2, pH = 7.4 and pH = 9.2 at 37 °C.

synthesized hydrogels at different pH values. Fig. 4a shows the release profile of model drug through Gg-*cl*-poly(NIPA-*co*-AA) and Gg-*cl*-poly(NIPA-*co*-AA)/-*o*-MWCNT, respectively. The effect of pH on metformin HCl release behaviour through Gg-*cl*-poly(NIPA -*co*-AA) and Gg-*cl*-poly(NIPA-*co*-AA)/-*o*-MWCNT (30 mg-GNACNT-3) has been studied as maximum drug release was observed for these hydrogel sample. From Fig. 4a it is evident that for the hydrogels GNACNT-0, GNACNT-1 and GNACNT-3 the cumulative drug release for metformin HCl was found to be about 5.22%, 47.54% and 58.07% at a pH of 1.2. While for the similar hydrogel samples the drug release was found to be 4.34%, 51.02% and 61.93% in additional basic media at pH = 7.4 while the release extended the value of 7.49%, 61.46% and 63.07% at pH = 9.2 after 24 h. The drug release was also discovered to be time dependent. Initially, the drug release was slow, but it increased over time, and after reaching the maximum, equilibrium was achieved with a steady flow of metformin HCl. As shown in Fig. 4a, small drug release was observed at the initial 2 h in 0.1 N HCl solution (pH 1.2), at the end of 2 h. On the other hand, the drug was readily released at higher pH of the loaded drug was released at the end of 24 h. The pH-dependent release of metformin HCl from Gg-*cl*-poly(-NIPA-*co*-AA)/-*o*-MWCNT (GNACNNT) based hydrogels might be attributed to the fact that, at acidic pH, the carboxyl groups of graft copolymer (GNACNT), used for the hydrogel formation, remain unionized and favour the formation of hydrogen bonding between carboxyl groups of GNACNT in acidic solution. This makes the polymer sections inflexible, which in turn, hinders water absorption, decreases swelling and hinders drug release. On the other hand, at alkaline pH (pH = 9.2), the carboxyl groups of GNACNT become ionized, and thereby, increase the repulsion between resultant carboxylate ions (COO^-), resulting in relaxation of copolymer chains with successive hydrogel swelling and significant drug release. The fractions of glucuronic acid, galacturonic acid and uronic acid present in virgin GG contribute towards carboxyl groups in grafted copolymer.

The release profile of sodium diclofenac model drug was investigated using synthesized hydrogels at different pH values. Fig. 4b shows the release profile of model drug through Gg-*cl*-poly(NIPA-*co*-AA) and Gg-*cl*-poly(NIPA-*co*-AA)/-*o*-MWCNT, respectively. The percentage drug release for sodium diclofenac was found to be about 0.92%, 0.95% and 3.59% at a pH of 1.2. While for the similar hydrogel samples the drug release was found to be 94.87%, 98.28% and 99.22% in additional basic media at pH = 7.4 while the release extended the value of 99.65%, 99.91% and 99.97% at pH = 9.2 after 24 h. Because –COOH groups on the polymeric chain are unionised at lower pH, resulting in the collapsed condition of the GNACNT hydrogel matrix, drug release was observed to increase with pH increase. Because these groups are largely ionised to $-COO^-$, the drug release rate was somewhat greater at higher pH. These ionic charges oppose one another, resulting in more drug diffusion from the hydrogel.[25] The drug release was greater at higher pH levels due to the ionisation of –COOH groups, and the strongest repulsions between distinct hydrogel chains occurred. As a consequence, the hydrogel's water absorbency increased, resulting in increased water absorption and, as a result, increased drug diffusion.[41] The drug release was also discovered to be time dependent. Initially, the drug release was slow, but it increased over time, and after reaching the maximum, equilibrium was achieved with a steady flow of metformin HCl. However, because of protonation at pH 1.2, functional groups of monomers formed conjugates with counterions, strengthening the polymeric structure of the hydrogel with strong hydrogen bonding. Because of the strong hydrogen bonding, there was little swelling and consequently little drug release.[42] Finally, we can show that at the low pH of 1.2, the hydrogel remained protonated/un-ionized due to the p*K*a values of its reagents, resulting in little swelling and drug release. As the pH varied between 1.2, 7.4, and 9.2, deprotonation/ionization of the polymer and monomer functional groups began, and hydrogel networks extended, causing swelling and drug release to rise.[43] Evidently, the copolymerization of NIPA with small amounts of AAc was extremely interesting since it

provided a novel material that can modulate drug release according to medium pH, acquiring a potential utility for administration of oral matrix systems. As is well known, it is occasionally important to protect the gastric pH (pH = 1.2) from particularly labile medications, permitting their release once they have passed through the stomach and into the gastro intestinal tract, where the pH rises dramatically. As a result, the NIPA:AAc material has potential biopharmaceutical features since it can load a high proportion of medication and adjust the release in simulated gastric fluid (SGF) or phosphate buffered saline (PBS) for the construction of oral delayed drug delivery systems.[20] As a result, the synthesised hydrogels can be employed in the building of controlled drug delivery systems where fast drug release is the objective initially and sustained release is desired afterwards.

3.4.2. Mathematical model for drug release study (metformin). The kinetics release mechanism of the metformin HCl drug from GNACNT-0, GNACNT-1 and GNACNT-3 hydrogel samples was assessed by fitting the *in vitro* release data on the mathematical equations of the Korsmeyer–Peppas, zero order,

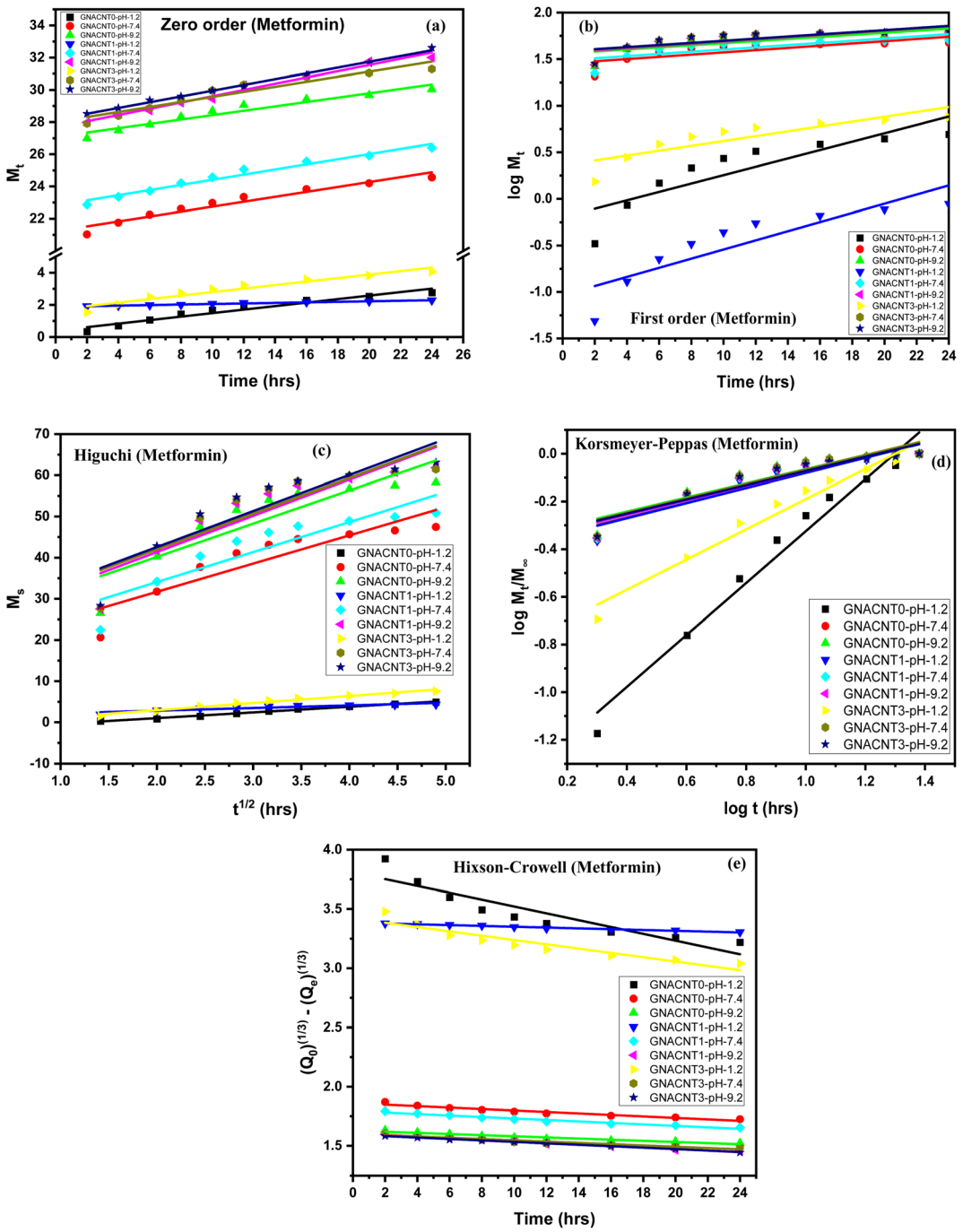

Fig. 5 Dispersed plots of metformin drug release data in different models (a) zero order, (b) first order, (c) Higuchi model, (d) Korsmeyer–Peppas and (e) Hixson-Crowell model.

Table 3 Korsmeyer–Peppas model drug release mechanism

Exponent (n)	Drug release mechanism
$n \leq 0.45$	Fickian diffusion (case I diffusional)
$0.45 < n < 0.89$	Anomalous (non-fickian) diffusion
$n = 0.89$	Zero order release (case II transport)
$n > 0.89$	Super case II transport

first order, Higuchi and Hixson-Crowell, (Fig. 5, Table 3). By determining the diffusional constant 'n' it is possible to gain information about the mechanism controlling water uptake or drug release from hydrogel. From the kinetic modeling data, drug release from hydrogel was found to follow Korsmeyer–Peppas model with R^2 value for metformin HCl was found to be in the range of 0.8432–0.9686. The Higuchi and zero-order models are mutually exclusive. Higuchi's model is consistent with Fick's law-based mass transport and is precisely applicable

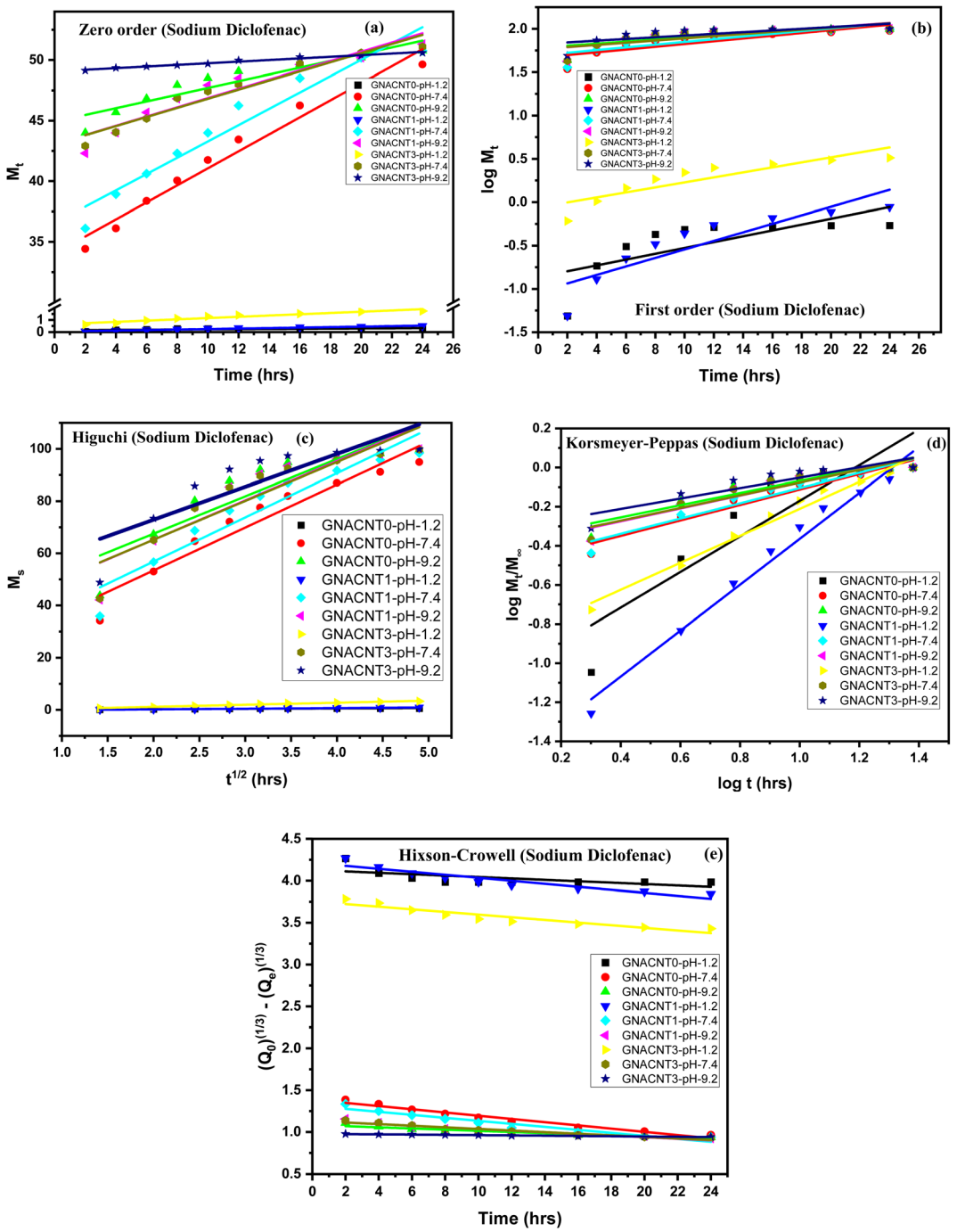

Fig. 6 Dispersed plots of sodium diclofenac drug release data in different models (a) zero order, (b) first order, (c) Higuchi model, (d) Korsmeyer–Peppas and (e) Hixson-Crowell model.

to polymer systems that do not exhibit swelling. The zero-order model, on the other hand, applies to systems in which swelling happens due to erosion or relaxation of the polymer matrix. The semi-empirical model of Korsmeyer and Peppas, on the other hand, may be used in conjunction with the zero-order model to explain the releasing processes. To find the best fit model, release profiles of the drug-loaded hydrogels produced were examined (figure) by utilizing various kinetic models and the values of the release constant and the correlation coefficient (R^2) were discovered. The ideal R^2 value for a best fit model is one that is closer to 1. For metformin HCl the R^2 value for the Higuchi model ranged from 0.75951 to 0.99246. For Korsmeyer–Peppas model the GNACNT-0 hydrogel sample the diffusion constant '*n*' has a value of 1.08914 ($n > 0.89$) indicating super case II transport whereas for GNACNT-1 hydrogel the '*n*' value is 0.30823 ($n \leq 0.45$) indicating Fickian diffusion (case I diffusional) and for GNACNT-3 hydrogel sample the '*n*' value is found to be 0.63371 ($0.45 < n < 0.89$) indicating the anomalous (non-Fickian) diffusion at a pH of 1.2. While for the same hydrogel samples at a pH of 7.4 and 9.2 all the hydrogel samples have '*n*' value ($n \leq 0.45$) indicating Fickian diffusion (case I diffusional).

3.4.3. Mathematical model for drug release study (sodium diclofenac). The kinetics release mechanism of the sodium diclofenac drug from GNACNT-0, GNACNT-1 and GNACNT-3 hydrogel samples was assessed by fitting the *in vitro* release data on the mathematical equations of the Korsmeyer–Peppas, zero order, first order, Higuchi and Hixson-Crowell, (Fig. 6 and Table 3). By determining the diffusional constant '*n*' it is possible to gain information about the mechanism controlling water uptake or drug release from hydrogel. From the kinetic modeling data, drug release from hydrogel was found to follow Korsmeyer–Peppas model with R^2 value for sodium diclofenac was found to be in the range of 0.79793–0.97837. The Higuchi and zero-order models are mutually exclusive. Higuchi's model is consistent with Fick's law-based mass transport and is precisely applicable to polymer systems that do not exhibit swelling. The zero-order model, on the other hand, applies to systems in which swelling happens due to erosion or relaxation of the polymer matrix. The semi-empirical model of Korsmeyer and Peppas, on the other hand, may be used in conjunction with the zero-order model to explain the releasing processes. To find the best fit model, release profiles of the drug-loaded hydrogels produced were examined (figure) by utilizing various kinetic models and the values of the release constant and the correlation coefficient (R^2) were discovered. The ideal R^2 value for a best fit model is one that is closer to 1. For sodium diclofenac the R^2 value for the Higuchi model ranged from 0.75951 to 0.99246. For Korsmeyer–Peppas model the GNACNT-0 hydrogel sample the diffusion constant '*n*' has a value of 0.91023 ($n > 0.89$) whereas for GNACNT-1 hydrogel the '*n*' value is 1.17309 ($n > 0.89$) where both the hydrogel samples indicating the super case II transport and for GNACNT-3 hydrogel sample the '*n*' value is found to be 0.68977 ($0.45 < n < 0.89$) indicating the anomalous (non-Fickian) diffusion at a pH of 1.2. While for the same hydrogel samples at a pH of 7.4 and 9.2 all the hydrogel samples have '*n*' value ($n \leq 0.45$) indicating Fickian diffusion (case I diffusional).

Table 4 Metformin HCl and sodium diclofenac drug release kinetics of GNACNT-0, GNACNT-1 and GNACNT-3 at different pH values (pH = 1.2, pH = 7.4 and pH = 9.2)

		Zero-order	First-order	Higuchi	Korsmeyer–Peppa's		Hixson-Crowell model
		M_t *vs.* t	$\log M_t$ *vs.* t	M_t/M_∞ *vs.* $t^{1/2}$	$\log(M_t/M_\infty)$ *vs.* $\log t$		$\sqrt[3]{Q_0} - \sqrt[3]{Q_t}$ *vs.* t
Kinetic models linear fit	pH	R^2	R^2	R^2	R^2	n	R^2
Metformin HCl							
GNACNT-0	(pH-1.2)	0.9397	0.75248	0.99246	0.96868	1.08914 ± 0.0691	0.82392
	(pH-7.4)	0.94104	0.52906	0.78919	0.86006	0.31306 ± 0.0442	0.93164
	(pH-9.2)	0.93238	0.72454	0.75951	0.8432	0.29598 ± 0.04461	0.92736
GNACNT-1	(pH-1.2)	0.98052	0.50381	0.83045	0.88754	0.31653 ± 0.03952	0.97794
	(pH-7.4)	0.96705	0.53619	0.79474	0.86479	0.30823 ± 0.04267	0.96214
	(pH-9.2)	0.97942	0.54547	0.80421	0.86965	0.30449 ± 0.04129	0.97781
GNACNT-3	(pH-1.2)	0.92305	0.71252	0.97364	0.96363	0.63371 ± 0.04343	0.86129
	(pH-7.4)	0.91155	0.51406	0.77038	0.85091	0.30105 ± 0.04407	0.90627
	(pH-9.2)	0.99439	0.53037	0.78795	0.85846	0.29768 ± 0.0423	0.99539
Sodium diclofenac							
GNACNT-0	(pH-1.2)	0.40601	0.44615	0.7999	0.80307	0.91026 ± 0.15698	0.33967
	(pH-7.4)	0.97062	0.66383	0.91654	0.94013	0.39464 ± 0.03507	0.95797
	(pH-9.2)	0.8501	0.50654	0.7647	0.8457	0.31073 ± 0.0464	0.83965
GNACNT-1	(pH-1.2)	0.96537	0.75248	0.99024	0.97837	1.17309 ± 0.06159	0.85815
	(pH-7.4)	0.93618	0.63829	0.89828	0.9272	0.38973 ± 0.03842	0.92143
	(pH-9.2)	0.89615	0.54272	0.80352	0.87037	0.32905 ± 0.04448	0.88407
GNACNT-3	(pH-1.2)	0.91632	0.75346	0.98029	0.97738	0.68977 ± 0.03704	0.86026
	(pH-7.4)	0.9372	0.5545	0.81402	0.8776	0.32347 ± 0.04234	0.9292
	(pH-9.2)	0.977	0.44371	0.69039	0.79793	0.26566 ± 0.04654	0.97649

Although R^2 is a goodness-of-fit measure for linear regression models, it sometimes is not enough to evaluate the difference if the R^2 values give close results. In the present study for GNACNT-3 hydrogel sample (pH = 9.2), zero order ([0.9944 for metformin HCl] and [0.977 for sodium diclofenac]) and Hixson-Crowell kinetics R^2 ([0.9954 for metformin HCl] and [0.9765 for sodium diclofenac]) values were also found so close to each other. According to the results, the metformin hydrochloride (R^2 = 0.99439) and sodium diclofenac (R^2 = 0.977) presented a high correspondence to the zero-order model for GNACNT-3 hydrogel sample (pH = 9.2), which means that the crystals were immediately eroded and dissolved. This behavior is a concern of the high hydrophilicity of the drug.[15]

Various kinetic models are fitted using the release data. These models working equations are listed in Table 3. The effectiveness of these models in fitting the kinetic data is seen in Fig. 5 and 6. Table 3 presents relatable regression values and release exponents Table 4.

4. Conclusions

In the current study, the -*o*-MWCNT was grafted onto Gg-*cl*-poly(NIPAm-*co*-AA) chains and copolymerized utilising *N*,*N*′-methylene-bis-acrylamide (MBA), ammonium persulfate (APS) and TEMED as a crosslinker, initiator system in an aqueous solution to generate the Gg-*cl*-poly(NIPAm-*co*-AA)/-*o*-MWCNT hydrogel. In this study, a novel Gg-*cl*-poly(NIPAm-*co*-AA)/-*o*-MWCNT (GNACNT) hydrogel was fabricated and challenged for its efficacy as a pH sensitive drug delivery system. GNACNT hydrogel was produced by free radical polymerization technique. The fabricated hydrogels were characterized chemically, morphologically. In conclusion, it can be stated that -*o*-MWCNT have successfully increased the hydrophobicity of all the acrylic acid grafted hydrogels through interaction with the matrix. The results of the metformin hydrochloride and sodium diclofenac drug release study showed that drug release was more favourable at pH 9.2, as the graft copolymer (hydrogel) used to make the drug-loaded hydrogel maintains the homogeneity of its carboxyl groups at basic pH and facilitates the formation of hydrogen bonds between them in basic solution. Both sodium diclofenac and metformin-loaded hydrogel conformed to Fickian diffusion. The hydrogel was found to be a good drug delivery device for both drugs in alkaline pH. The results showed that the synthesized hydrogels combinations could be employed as potential agents for controlled drug delivery vehicles where the fast release of the drug is compulsory at early stages and controlled release at later stages.

In conclusion, the present study successfully demonstrated the synthesis and *in vitro* evaluation of a novel biodegradable Gg-*cl*-poly(NIPAm-*co*-AA)/-*o*-MWCNT hydrogel for the combined delivery of metformin and sodium diclofenac. The developed hydrogel exhibited promising physicochemical properties and sustained release profiles of both drugs, indicating its potential as an effective drug delivery system.

However, the current study is just the initial step towards harnessing the full potential of this drug delivery platform. Several avenues for future research and development exist to enhance the understanding and applicability of the hydrogel-based system such as *in vivo* studies; optimization of drug release kinetics; biocompatibility and toxicity studies; combination with other therapeutic agents; incorporation of targeting strategies; scale-up and manufacturing considerations and long-term stability studies.

Conflicts of interest

There are no conflicts to declare.

Acknowledgements

The authors are highly thankful to SHODH, for providing fellowship and contingency to one of the authors for carrying out the research work. The authors are also thankful to Department of Chemistry, Sardar Patel University, Vallabh Vidyanagar for laboratory facility and CISST Department for characterization of the samples.

References

1 S. Kausar, A. Erum, U. R. Tulain, M. A. Hussain, M. Farid-Ul-Haq, N. S. Malik and A. Rashid, *Adv. Polym. Technol.*, 2021, **2021**, 1–17.
2 U. R. Tulain, M. Ahmad, A. Rashid, M. Z. Malik and F. M. Iqbal, *Adv. Polym. Technol.*, 2018, **37**, 290–304.
3 H. Idrees, S. Z. J. Zaidi, A. Sabir, R. U. Khan, X. Zhang and S. U. Hassan, *Nanomaterials*, 2020, **10**, 1–22.
4 S. Raveendran, A. K. Rochani, T. Maekawa and D. S. Kumar, *Materials*, 2017, **10**, 929–969.
5 R. Song, M. Murphy, C. Li, K. Ting, C. Soo and Z. Zheng, *Drug Des., Dev. Ther.*, 2018, **12**, 3117–3145.
6 R. R. Bhosale, R. A. M. Osmani, A. S. Abu Lila, E. S. Khafagy, H. H. Arab, D. V. Gowda, M. Rahamathulla, U. Hani, M. Adnan and H. V. Gangadharappa, *RSC Adv.*, 2021, **11**, 14871–14882.
7 R. Ali, M. Osmani, E. Singh, K. Jadhav, S. Jadhav and R. Banerjee, *Appl. Adv. Green Mater.*, 2020, 573–630.
8 A. M. Wagner, D. S. Spencer and N. A. Peppas, *J. Appl. Polym. Sci.*, 2018, **46154**, 1–17.
9 H. Sun, L. Yang, M. P. Thompson, S. Schara, W. Cao, W. Choi, Z. Hu, N. Zang, W. Tan and N. C. Gianneschi, *Bioconjugate Chem.*, 2019, **30**, 1889–1904.
10 V. Pillay, A. Seedat, Y. E. Choonara, L. C. Du Toit, P. Kumar and V. M. K. Ndesendo, *AAPS PharmSciTech*, 2013, **14**, 692–711.
11 M. Mahesh Reddy, D. Jagadeeswara Reddy, A. Moin and H. G. Shivakumar, *Pharm. Lett.*, 2011, **3**, 119–128.
12 M. Kaur and M. Datta, *Adsorpt. Sci. Technol.*, 2014, **32**, 365–387.
13 M. Saravanan, K. Bhaskar, G. Maharajan and K. S. Pillai, *Int. J. Pharm.*, 2004, **283**, 71–82.
14 L. M. Himiniuc, R. Socolov, I. Nica, M. Agop, C. Volovat, L. Ochiuz, D. Vasincu, A. M. Rotundu, I. A. Rosu, V. Ghizdovat and S. R. Volovat, *Gels*, 2023, **9**(5), 422.

15 T. S. da Silva, D. A. K. Silva and A. L. Nogueira, *J. Appl. Polym. Sci.*, 2021, 138.
16 T. M. Don, M. L. Huang, A. C. Chiu, K. H. Kuo, W. Y. Chiu and L. H. Chiu, *Mater. Chem. Phys.*, 2008, **107**, 266–273.
17 M. C. I. Mohd Amin, N. Ahmad, N. Halib and I. Ahmad, *Carbohydr. Polym.*, 2012, **88**, 465–473.
18 N. Milašinović, M. Kalagasidis Krušić, Z. Knežević-Jugović and J. Filipović, *Int. J. Pharm.*, 2010, **383**, 53–61.
19 M. E. Mc neill and N. B. Graham, *J. Biomater. Sci., Polym. Ed.*, 1996, **7**, 937–951.
20 J. C. Cuggino, C. B. Contreras, A. Jimenez-Kairuz, B. A. Maletto and C. I. Alvarez Igarzabal, *Mol. Pharmaceutics*, 2014, **11**, 2239–2249.
21 B. Kamaliya, P. N. Dave and P. M. Macwan, *J. Appl. Polym. Sci.*, 2022, **139**, 1–16.
22 K. Sharma, V. Kumar, B. Chaudhary, B. S. Kaith, S. Kalia and H. C. Swart, *Polym. Degrad. Stab.*, 2016, **124**, 101–111.
23 C. Siangsanoh, S. Ummartyotin, K. Sathirakul, P. Rojanapanthu, W. Treesuppharat, S. Ummartyotin, K. Sathirakul, P. Rojanapanthu and W. Treesuppharat, *J. Mol. Liq.*, 2018, 1–43.
24 B. S. Kaith, Saruchi, R. Jindal and M. S. Bhatti, *Soft Matter*, 2012, **8**, 2286–2293.
25 Saruchi, B. S. Kaith, R. Jindal, V. Kumar and M. S. Bhatti, *RSC Adv.*, 2014, **4**, 39822–39829.
26 R. Das and S. Pal, *Colloids Surf., B*, 2013, **110**, 236–241.
27 D. Das, R. Das, P. Ghosh, S. Dhara, A. B. Panda and S. Pal, *RSC Adv.*, 2013, **3**, 25340–25350.
28 D. Das, R. Das, J. Mandal, A. Ghosh and S. Pal, *J. Appl. Polym. Sci.*, 2014, **131**, 1–12.
29 R. Gendle, B. Kaushik, S. Verma, R. Patel, S. K. Singh and K. P. Namdeo, *Int. J. ChemTech Res.*, 2010, **2**, 4–10.
30 Y. Liu, Y. Sui, C. Liu, C. Liu, M. Wu and B. Li, *Carbohydr. Polym.*, 2018, **188**, 27–36.
31 S. Sethi, B. S. Kaith, M. Kaur, N. Sharma and S. Khullar, *J. Biomater. Sci., Polym. Ed.*, 2019, **30**, 1687–1708.
32 G. Shelar-Lohar and S. Joshi, *RSC Adv.*, 2019, **9**, 41326–41335.
33 E. Titus, N. Ali, G. Cabral, J. Gracio, P. Ramesh Babu and M. J. Jackson, *J. Mater. Eng. Perform.*, 2006, **15**, 182–186.
34 C. A. Dyke and J. M. Tour, *J. Phys. Chem. A*, 2004, **108**, 11151–11159.
35 J. L. Bahr, J. Yang, D. V. Kosynkin, M. J. Bronikowski, R. E. Smalley and J. M. Tour, *J. Am. Chem. Soc.*, 2001, **123**, 6536–6542.
36 S. Chen, L. Jiang and D. Yi, *J. Appl. Polym. Sci.*, 2011, **121**(6), 3322–3331.
37 R. P. Swain, R. Nagamani and S. Panda, *J. Appl. Pharm. Sci.*, 2015, **5**, 94–102.
38 Z. E. Ee, G. Mm, S. Gad and H. A. Yassin, *Int. J. Adv. Pharm., Biol. Chem.*, 2015, **4**, 330–335.
39 Y. Pore, V. Mangrule, M. Mane and A. Chopade, *Asian J. Pharm. Pharmacol.*, 2017, **3**, 208–214.
40 N. Gull, S. M. Khan, O. M. Butt, A. Islam, A. Shah, S. Jabeen, S. U. Khan, A. Khan, R. U. Khan and M. T. Z. Butt, *Int. J. Biol. Macromol.*, 2020, **162**, 175–187.
41 K. Sharma, V. Kumar, B. Chaudhary, B. S. Kaith, S. Kalia and H. C. Swart, *Polym. Degrad. Stab.*, 2016, **124**, 101–111.
42 K. Sohail, I. U. Khan, Y. Shahzad, T. Hussain and N. M. Ranjha, *Braz. J. Pharm. Sci.*, 2014, **50**, 173–184.
43 M. Suhail, Y. F. Shao, Q. L. Vu and P. C. Wu, *Gels*, 2022, **8**(3), 155.